Coaxial Nanotubes of Stimuli Responsive Polymers with Tunable Release Kinetics

SCHOLARONE™
Manuscripts

Coaxial Nanotubes of Stimuli Responsive Polymers with Tunable Release Kinetics

Efe Armagan[1], Gozde Ozaydin Ince[1,2*]

[1]*Materials Science and Nanoengineering Program, Faculty of Engineering and Natural Sciences, Sabanci University, 34956 Istanbul, Turkey*
[2]*Sabanci University Nanotechnology Research and Application Center, 34956 Istanbul, Turkey*

*Corresponding Author:
E-mail: gozdeince@sabanciuniv.edu
Phone: +90(216) 483 9878
Address: Sabanci University, Orta Mahalle, Universite Caddesi No: 27, Orhanlı, 34956 Istanbul, Turkey

Abstract:

Stimuli responsive polymeric (SRP) nanotubes have great potential as nanocarriers of macromolecules due to their large surface areas and release mechanisms that can be activated externally. In this work, we demonstrate vapor phase synthesis of coaxial nanotubes with layers of different SRP polymers for improved release kinetics. Temperature responsive poly(N-isopropylacrylamide) (pNIPAAm), pH responsive poly(Methacrylic acid) (pMAA) and poly(Hydroxyethly methacrylate) (pHEMA) are used to fabricate the responsive coaxial nanotubes and the phloroglucinol dye is used as the model molecule to study the release kinetics. Fastest release is observed with single layer pNIPAAm nanotubes with rates of 0.134 min^{-1}, whereas introducing pHEMA or pMAA as inner layers slows the release, enabling tuning of the response. Furthermore, repeating the release studies multiple times show that the release rates remain similar after each run, confirming the stability of the nanotubes.

INTRODUCTION

In recent years, nano-sized materials have become important tools in various applications, especially in biotechnology[1,2] and food industry[3,4]. Fabrication of these nanostructures from polymers has major advantages due to low cost, ease of fabrication and high biocompatibility, significantly increasing interest in different polymeric systems and synthesis methods[5,6].

Stimuli Responsive Polymers (SRP) are polymers whose physical properties change with environmental stimuli such as temperature, pH, moisture/water and light[7]. The SRP based release systems benefit from the stimuli triggered response of these nanostructures to control the release kinetics. SRP nanostructures of different shapes; i.e. nanospheres[8,9,10], nanorods[11,12] or nanotubes[13,14,15], are generally fabricated via conventional solution polymerization techniques, such as precipitation polymerization[16,17]. On the other hand, conformal coatings on high aspect ratio surfaces and lack of solvents during synthesis are major advantages of the vapor phase polymerization techniques, making them preferable for some specific applications.

Initiated chemical vapor deposition (iCVD) is a vapor phase polymer deposition technique based on free-radical polymerization. All the monomer and initiator molecules are delivered in gas phase to the vacuum reactor. The monomer directly adsorb on the surface of the cooled substrate, whereas initiator molecules are thermally decomposed by heated filaments forming radicals. These radicals then react with the monomer molecules initiating the surface polymerization[18]. Surface polymerization, not only enables depositions of highly crosslinked polymers, but also helps to achieve high degrees of conformality. We have demonstrated

fabrication of functional nanotubes using templated iCVD technique where a porous template was utilized to synthesize the tubular polymeric nanostructures[19]. We reported fabrication of nanotubes with different crosslink ratios to control swelling properties[20], as well as nanotubes that release their cargo when triggered by temperature[21] or pH changes[22]. In this study, we report fabrication of single layer poly(N-isopropylacrylamide) (pNIPAAm), coaxial pNIPAAm-poly(Methacrylic Acid) pMAA and coaxial pNIPAAm- poly (Hydroxyethly methacrylate) pHEMA nanotubes whose molecule loading and release rates could be controlled by tuning their chemical composition.

PNIPAAm is a thermoresponsive polymer which demonstrates a phase segregation above the lower critical solution temperature (LCST) of approximately 32°C [23,24]. Below LCST, hydrogen bonds form between the hydrophilic amide groups and water molecules, whereas above LCST the hydrogen bonds form between the amide groups of the pNIPAAm chains exposing the hydrophobic isopropyl groups[25]. This transition from hydrophilic to hydrophobic behavior above LCST can be used as a trigger in controlled release mechanisms, making pNIPAAm one of the most commonly used polymers in drug delivery applications[26]. Studies focusing on drug delivery applications of pNIPAAm generally involve bulk polymers or nanospheres, loaded with drug that is released as the polymer shrinks when heated[27,28,29]. Although nanotubular structures have advantages of large surface to volume ratios, reports on pNIPAAm nanotubes are limited due to challenging fabrication techniques[30,31,32].

Ability to trigger physical changes of nanotubes using multiple stimuli, provides better control of the release rates. In this study, coaxial nanotubes of pNIPAAm-pH responsive pMAA

and pNIPAAm -pHEMA were fabricated and their response to pH and temperature changes was studied. Earlier studies generally report coaxial nanotubes fabricated by e-spinning technique[33,34,35]. However, studies on coaxial nanotubes of stimuli responsive polymers are very limited. In this report, we introduce templated iCVD as an effective technique to fabricate polymeric coaxial nanotubes and we aim to tune the release rates by incorporating different SRPs in the nanotubes. In this first part of the paper, we demonstrate upload and release performance of single layer pNIPAAm nanotubes and in the second part, we report coaxial nanotubes of SRP and discuss the effects of multiple stimuli on the response.

Experimental

Nanotube sample preparation:

AAO templates and flat Si substrates were coated with crosslinked pNIPAAm, pNIPAAm+pHEMA or pNIPAAm+pMAA, pEGDMA polymers using iCVD. PEGDMA polymer was used to fabricate the control samples. Si wafers and AAO templates were coated simultaneously; placed next to each other in the chamber. Flat Si substrates were used for chemical identification whereas AAO templates were used for nanotube fabrication.

The monomers NIPAAm (Aldrich, 97%), MAA (Aldrich, 99%), HEMA (Aldrich, 99%), the crosslinker ethylene glycol dimethacrylate (EGDMA, Aldrich, 98%) and the initiator tert-butyl peroxide (TBPO, Aldrich, 98%) were used as received, without further purification. NIPAAm, MAA, HEMA and EGDMA monomers were heated up to $80^{o}C$, $75^{o}C$, $70^{o}C$, $85^{o}C$ respectively, in jars outside the chamber and delivered into the system in the vapor phase. For all depositions, the substrate and filament temperatures were $35°C$ and $240°C$, respectively and the chamber pressure was maintained at 450 mTorr. Flowrates of monomers for different polymer depositions

were varied between 0.1 and 1 sccm. Details of deposition conditions are given in Table 1 (Supporting Information).

After depositions, coated AAO templates were immersed in 1 M HCl solution for 24 hours, which etched the AAO template without damaging the polymer layer. The polymer nanotubes were released by removal of the AAO template. For the fabrication of closed-end nanotubes, the coated AAO templates were first loaded with dye molecules, and another layer of polymer was deposited on top to cap the tube openings. Finally, the templates were etched by immersing in HCl solution.

For coaxial nanotubes deposition, two different types of polymers were subsequently coated inside AAO. The thickness of each polymer layer was measured to be approximately 15 nm for all polymer depositions. The overall wall thicknesses of the coaxial and single layered nanotubes were, therefore fixed at 30 ± 5nm. For comparison, thicker nanotubes of single layer pNIPAAm and coaxial pNIPAAm+pMAA nanotubes were fabricated, with wall thicknesses of 50 ± 10nm. For pNIPAAm+pHEMA coaxial nanotubes with pNIPAAm outer layer and pHEMA inner layer, pNIPAAm polymer was coated first, followed by a plasma etching process to remove the excess polymer on the AAO pore openings. PHEMA layer was deposited following the etching. For pNIPAAm+pMAA coaxial nanotubes with pNIPAAm outer layer and pMAA inner layer, similar deposition and plasma etching process was used. As the final step in the fabrication process, the AAO templates with double polymer layers were etched in HCl solution as detailed earlier. In all polymer depositions, EGDMA was used as the crosslinker.

Characterization of the nanotubes:

The chemical analysis of the nanotubes was done using Fourier Transform Infrared Spectroscopy (FTIR) (Thermo Fischer Scientific, Model NICOLET iS10). The spectra were acquired at 4 cm^{-1} resolution and the number of scans were 256. Field Emission Scanning Electron Microscope (Zeiss, SUPRA VP 35) was used to image the nanotubes at 4 kV accelerating voltage.

The swelling response of the polymer thin films on flat Si wafer was analyzed using a spectroscopic ellipsometer (M-2000, J.A. Woolam) equipped with liquid cell. The dynamic measurements were done at 75° within the wavelength range of 300-800 nm. Swelling measurements of pNIPAAm and pHEMA films were performed at 40°C with DI water whereas HCl solution (pH=4) was used on pMAA coated Si wafer to see the effect of pH change on the swelling. Thickness change was monitored for 60 minutes and the swelling ratio was calculated according to Cauchy model fitting.

Loading and release studies:

The performance of the polymer nanotubes as molecular carriers was studied using the model dye Phloroglucinol (Phl), which has UV excitation peak at 267 nm. For loading experiments, the nanotubes were immersed in 0.003 M Phl dye solution for 24 hours at different temperatures and pH conditions. The Phl solution was prepared with DI water and the pH of the solution was adjusted using KOH. At the end of 24 hours, the dye concentration in the solution was measured by UV-Vis spectroscopy and the concentration of the loaded dye was calculated.

After the loading, the nanotube samples were rinsed three times with DI water to remove the excess dye solution before the release experiments. For the closed-end nanotubes, loading was performed prior to etching of the AAO template.

For the release experiments, the polymer nanotubes were immersed in DI water at different temperature and pH conditions. The change in the dye concentration in water was monitored by taking 6 ml of solution and measuring the concentration using UV-Vis periodically over time. The stability studies were performed by repeating the loading and release experiments 3 times for each set of samples and the change in the release performance of the polymer nanotubes was monitored. The details of the loading and release conditions are detailed in Table 1.

Results and Discussion

FTIR analysis of iCVD deposited polymers on Si wafers confirms the successful copolymerization of NIPAAm, MAA and HEMA with EGDMA as shown in Fig. 1. The peaks at 3300 cm^{-1}, 1530 cm^{-1} and 1630 cm^{-1} correspond, respectively, to the N-H stretching vibration, C-N-H bending vibration and C=O vibration of NIPAAm[36]. On the other hand, the broad peak between 3150 cm^{-1}-3550 cm^{-1} is due to O-H stretching vibration and the peak at 1730 cm^{-1} is due to the C=O stretching vibration of HEMA[37]. The peak at 1700 cm^{-1} corresponds to the C=O stretching vibration of MAA, whereas C=O stretching vibration of EGDMA is at 1730 cm^{-1}. The absence of a peak between 1600-1650 cm^{-1} confirms the complete polymerization of the monomer adsorbed on the surface. The EGDMA content in the deposited films can be calculated from the ratios of the characteristic peak areas of the monomers. For the polymer systems used in

this study EGDMA content in the films are calculated as 22.9%, 32.1% and 56.5% for pNIPAAm, pHEMA and pMAA, respectively.

The SEM images of the coaxial nanotubes NIMA are shown in Fig. 2(a). Due to the similarity in their polymer structure, the inner and outer layers cannot be distinguished in the SEM. The SEM images show that the nanotubes are approximately 200 nm in diameter and 10-20 μm in length. The tubes are hollow inside with 30 ± 5 nm of wall thickness (Fig. 2(b)). The SEM images of NIMA samples with wall thicknesses of 50 ± 10 nm and NIMA samples with closed ends are shown in Fig. 2(c) and Fig. 2(d), respectively.

Mesh size, ξ, of the deposited polymer nanotubes in their swollen and collapsed states, which affects the diffusion of the dye molecules through the polymer matrix, can be calculated using[38,39,40]:

$$\xi = Q^{\frac{1}{3}} \left[2C_n \left(\frac{M_c}{M_r} \right) \right]^{\frac{1}{2}} l \qquad \text{Eq. (1)}$$

where □ is the swelling ratio obtained from ellipsometer studies, l is C-C bond length (0.154 nm), C_n is characteristic ratio, M_r is the molecular weight of the monomer and M_c is the average molecular weight between the crosslinks. M_c can be calculated as following [40]:

$$\frac{1}{M_c} = \frac{2}{M_n} - \frac{\frac{v}{V_1}[ln(1-v_s)+v_s+x(v_s^2)]\left[1-\frac{M_r}{2M_c}v_s^{\frac{2}{3}}\right]^3}{\left(v_s^{\frac{1}{3}}-0.5v_s\right)\left[1+\frac{M_r}{2M_c}v_s^{\frac{1}{3}}\right]^2} \qquad \text{Eq. (2)}$$

where □ is specific volume of the polymer, □ is the Flory-Huggins interaction parameter, V_1 is the molar volume of water (18 cm^3/mol), □$_s$ is the ratio of dry thickness to wet thickness (given as 1/ □) and M_n is number average molecular weight of polymer. As, M_n is significantly larger

8

than M_c, the first term on the right can be ignored. The Flory-Huggins interaction parameters are assumed to be constant for different crosslink ratios within the range of $\square_s$ values obtained.

For pNIPAAm the values of C_n, M_r, $\square$ and $\square$ used in these equations are, respectively, 11.7, 113.16 g/mol, 0.909 cm³/g[41] and $\square$ is 0.51 for NIPAAM-water interaction[42]. For pHEMA the value of C_n is 6.9 [43], M_r is 130.14 g/mol, $\square$ is 0.931 cm³/g and $\square$ is 0.8 for pHEMA-water interaction[44]. Finally, for pMAA, C_n is 14.6 for MAA[45], M_r is 86.09 g/mol, $\square$ is 0.984 cm³/g and $\square$ is 0.59 for pMAA-water interaction. Table 2 shows the mesh size values of each polymer system calculated using Eq. (2).

The loading and release of Phl molecules from the polymer nanotubes were systematically studied using UV-Vis characterization, details of which were given earlier. The Phl dye molecules that are used in these studies have a solvent excluded volume[46] of 90.42 $\overset{o}{A}{}^3$, which corresponds to an approximate diameter of 5.7 $\overset{o}{A}$, smaller than the mesh sizes of the studied polymers. Figure 3 shows the released dye percentages as a function of time for different samples. As the loaded dye amount depends strongly on the amount of nanotubes in the solution, the loading concentrations may differ between samples; therefore, percentages are used to compare different samples. In none of the samples tested, release percentages higher than 50% could be obtained, which can be explained by the hydrophilic dye molecules being entrapped in the polymer mesh of the hydrophilic nanotubes. As for the control samples, pEGDMA nanotubes, which are not responsive to pH or temperature changes, are used.

The following experimental results were obtained with open-ended nanotubes. At the end of 120 minutes, 42.1% of the dye loaded was released by NI3, whereas only 3.2% and 4.3% were released by NI1 and NI2, respectively (Fig. 3(a)). The difference in the release percentages of NI1 and NI2 samples was insignificant and did not depend on the loading percentages. The significant difference in the release percentages between NI3 and other samples can be attributed to the hydrophobic nature of the pNIPAAM polymer at high temperatures; above the LCST of 32°C, indicating that low surface energy of the polymer nanotubes at high temperatures increased the release of the Phl molecules. The lower release percentages at 25°C, on the other hand, are due to hydrophilic interactions between the dye molecules and the pNIPAAM polymer. The release from the control samples is observed to be less than 2% due to the non-responsive nature of the pEGDMA nanotubes.

As for NIHE samples with pHEMA inner layer, 2.7%, 2.4% and 48.9% of the loaded dye was released by NIHE1, NIHE2 and NIHE3 (Fig. 3(b)). Same experimental conditions were applied to NIHE samples as that of NI samples. Considering that pHEMA polymer is not temperature responsive, release behavior similar to that of NI samples was observed, such that release increased at high temperatures and was independent from the loading temperatures.

For a better control of the release kinetics, another responsive polymer, pMAA, was used as the inner layer of the NIMA coaxial nanotubes. Changing the pH of the medium had effect on the release kinetics of NIMA samples where pMAA inner layer is the pH responsive polymer; which is hydrophilic at high pH values and hydrophobic at low pH values. At the end of 120 minutes, 2.93%, 2.31% and 43.9% of the loaded Phl was released by NIMA1, NIMA2 and NIMA3,

respectively (Fig. 3(c)). Loading experiments were performed at high pH conditions, where

pMAA polymer is hydrophilic, to improve the loading of the hydrophilic dye due to hydrophilic-

hydrophilic interaction between the dye molecules and the polymer. Release experiments, on the

other hand, were performed at low pH values where the polymer is hydrophobic, enhancing the

release of the hydrophilic dye molecules. Maximized release percentages with the NIMA coaxial

nanotubes were observed at low pH values and high temperatures, where both inner pMAA and

outer pNIPAAm layers were hydrophobic. When the outer layer was hydrophilic, the release

percentages decreased significantly, as observed with NIMA1 and NIMA2.

For all the samples studied, the highest release percentages obtained were less than 50%. This

can be attributed to dye molecules that are trapped between adjacent nanotubes, and which are

not washed off during the rinsing procedure. Although these dye molecules may be released

during unloading, they are not expected to have a big impact on the overall release percentages.

The burst release observed as a result of changes in the stimuli suggests that mostly dye

molecules that are loaded inside the nanotubes are released and the release is mainly through the

tube openings. The release of the dyes attached on the walls would be less affected by the

changes in the stimuli and would be at a slower rate than observed for burst release. Comparing

the percentage of dyes released from different polymers, the highest release percentage of 48.9%

was obtained with NIHE3, whereas the release percentages of NI3 and NIMA3 were similar and

42.1% and 43.9%, respectively. The lower release percentages of the NI3 and NIMA3 compared

to that of NIHE3 may be related to the smaller mesh sizes of pMAA and pNIPAAm when

collapsed. Mesh sizes of approximately 0.7 nm and 0.8 nm of pNIPAAm and pMAA in the

hydrophobic state are close to the size of Phl dye (0.57 nm). Therefore, the dye molecules

diffusing through the polymer mesh in the nanotube walls are trapped when the polymer

collapses. On the other hand, pHEMA has a mesh size of 1 nm at all conditions and this larger mesh size compared to the size of the dye molecules enables the release of the dye molecules through the nanotubes walls, as well.

The dominant release mechanism can be determined by comparing the release percentages of the open and closed end nanotubes. The release of the dye molecules from closed-end nanotubes is mainly via diffusion through the polymer mesh, whereas in open-ended nanotubes, bulk release of dyes from the tube openings is also active. The results showed that NIMA3 nanotubes with closed ends had release percentages of $10 \pm 4\%$ while NIMA3 samples with open ends had $40 \pm 2\%$ release. Higher release percentages indicate that the release is mainly from the open ends of the nanotubes activated by changes in the polymer wall dimensions.

The kinetics of the release from the nanotubes was studied by using the empirical formula:

$$x(t) = x_f(1 - e^{-kt}) \hspace{2cm} \text{Eq. (3)}$$

where x_f is the final Phl release percentage, $x(t)$ is release percentage at time t and k is the rate constant. The time release data of NI3, NIHE3 and NIMA3 can be fit to Eq. (3) in order to find the rate constants, k (Figure 3(a-c) dotted lines). From the fits, the rate constants k are found as 0.134 min^{-1}, 0.052 min^{-1} and 0.089 min^{-1} for NI3, NIHE3 and NIMA3, respectively. The significantly faster release kinetics observed with NI3 can be attributed to the hydrophobic nature of pNIPAAm at the release temperatures of 40°C. At high temperatures, the hydrophilic Phl molecules are released faster from hydrophobic pNIPAAm polymer. On the other hand, low release rate of NIHE3 is due to the hydrophilic nature of pHEMA polymer both at low and high temperatures. Although the larger mesh size of the pHEMA layer facilitates the process

increasing the amount of dye molecules released, the hydrophilic nature of the polymer, slows the rate of the dye release from the nanotubes. Therefore, burst-type release is not observed with NIHE3 nanotubes.

NIMA3 samples, on the other hand, demonstrate release kinetics that is faster than NIHE3, due to hydrophobic nature of pMAA at low pH values, leading to the collapse of the inner polymer layer. However, the release rates of NIMA3 are slower than that of NI3 although both samples are hydrophobic during release of the dye molecules. The collapse rates of pNIPAAm and pMAA thin films are 0.15 min^{-1} and 0.12 min^{-1}, respectively, as measured by the ellipsometer. The slow collapse rates of pMAA compared to pNIPAAm, may explain the lower release rates of NIMA3 than that of NI3. Although both NIMA3 and NI3 collapse, the slower response of the inner layer of NIMA3 results in lower dye release rates compared to NI3.

Nanotubes with thicker walls (~50 nm) generally have lower release percentages and slower kinetics. Release percentages of 31.9% and release rates of 0.06 min^{-1} were obtained with NI3 samples with thicker walls, whereas for thinner samples release percentages and rates were 42.1% and 0.13 min^{-1}, respectively. Similarly, NIMA3 samples with thicker and thinner walls had release percentages of 28.6% and 43.9% and release rates of 0.05 min^{-1} and 0.09 min^{-1}, respectively. As discussed earlier, although the dominant release mechanism is burst release from the tube openings, the lower rate constants obtained with nanotubes of thicker walls suggest that diffusion through the polymer mesh is also an active release mechanism. Furthermore, as the wall thickness increases, amount of dye molecules trapped within the polymer mesh increases, leading to reduced release percentages.

In order to study the stability of the nanotubes, the same experiments were repeated for three times and the release percentages as a function of time for each cycle were monitored. Figure 4 shows the release percentages at the end of 120 minutes for NI, NIHE and NIMA coaxial nanotubes after each cycle. In all samples, a drop in the overall release percentage of less than 10% was observed after each cycle, indicating an accumulation of dye molecules in the nanotubes, which can be due to the hydrophilic interactions between the dye molecules. The dye release rates of the nanotubes did not change significantly between cycles, confirming that the stimuli-responsive nature of the polymers was maintained.

The main aim in this study was to design coaxial nanotubes with controllable release kinetics. Our previous studies with single component stimuli responsive nanotubes showed that burst release of loaded molecules could be achieved in response to changes in the stimuli. However, release rates depend heavily on the polymers. The release rates of 0.089 min^{-1} and 0.13 min^{-1} were obtained with single layer pMAA[22] and pNIPAAm nanotubes, respectively, confirming the strong dependence of the release kinetics on the polymers used. In the current study, released rates ranging between 0.052 min^{-1} and 0.134 min^{-1} were achieved, confirming that by combining two stimuli responsive polymers in one system, release rates could be tuned.

Conclusions:

In conclusion, stimuli responsive polymeric nanotubes are fabricated using templated iCVD technique and the release of a model dye from these nanotubes is systematically studied. The

conformal nature of the iCVD process enables fabrication of coaxial nanotubes with layers of different stimuli responsive polymers. The release rates of the polymeric nanotubes depend on the polymers used to fabricate different layers. While pNIPAAm nanotubes have faster release rates, coaxial nanotubes with pMAA inner layers demonstrate slower release due to the difference in the swelling rates of the polymers. These results show that the release rates of the nanotubes can be tuned for different applications by designing coaxial nanotubes of SRP polymers. The amount of dye released, on the other hand, is approximately 50% of the loaded amount. This low performance can be attributed to the trapping or accumulation of the dye molecules inside the nanotubes, which needs to be improved by tailoring the mesh sizes of the polymers.

REFERENCES

[1] A. K. Gaharwar, N. A. Peppas and A. Khademhosseini, *Biotechnology and Bioengineering,* 2014, **111**, 441-453.

[2] N. Rapoport, *Prog. Polym. Sci.,* 2007, **32**, 962-990.

[3] S. F. Peteu, F. Oancea, O. A. Sicuia, F. Constantinescu and S. Dinu, *Polymers,* 2010, **2**, 229-251.

[4] H. M. C. Azeredo, L. H. C. Mattoso and T. H. McHugh, in *Advances in Diverse Industrial Applications of Nanocomposites,* ed. B. Reddy, In Tech, 2011, DOI: 10.5772/14437.

[5] F. S. Du, Y. Wang, R. Zhang and Z. C. Li, *Soft Matter*, 2010, **6**, 835-848.

[6] J. Chen, F. Wang, Q. Liu and J. Du , *Chem. Comm.*, 2014, **50**, 14482-14493.

[7] J. Hu, H. Meng, G. Li and S. I. Ibekwe, *Smart Mater. Struct.*, 2012 ,**21**, 053001-053024.

[8] Z. Deng, Z. Zhen, X. Hu, S. Wu, Z. Xu and P. K. Chu, *Biomaterials,* 2014, **32**, 4976-4986.

[9] H. Wang and G. L. Rempel, *Journal of Polymer Science, Part A: Polymer Chemistry,* 2013, **51**, 4440-4450.

[10] A. Arizaga, G. Ibarz and R. Pinol, *Journal of Colloid and Interface Science,* 2010, **348**, 668-672.

[11] S. Giri, B. G. Trewyn, M. P. Stellmaker and V. S. Y. Lin, *Angew. Chem. Int. Ed.,* 2005, **44**, 5038-5044.

[12] K. C. Hribar, M. H. Lee, D. Lee and J. A. Burdick, *American Chemical Society Nano,* 2011, **5**, 2948-2956.

[13] G. L. Li, Z. Zheng, H. Möhwald and D. G. Shchukin, *American Chemical Society Nano,* 2013, **7**, 2470-2478.

[14] G. Chen, R. Chen, C. Zou, D. Yang and Z. S. Chen, *J. Mater. Chem.,* 2014, **2**, 1327-1334.

[15] X. Chen,H. Chen, C. Tripisciano, A. Jedrzejewska, M. H. Rümmeli, R. Klingeler, R. J. Kalenczuk, P. K. Chu and E. B. Palen, *Chem. Eur. J.,* 2011, **17**, 4454-4459.

[16] G. L. Li, H. Möhwald and D. G. Shchukin, *Chem. Soc. Rev.*, 2013, **42**, 3628-3646.

[17] M.-H. Dufresne, D. Le Garrec, V. Sant, J.-C. Leroux and M. Ranger, *Int. J. Pharm.,* 2004, **277**, 81-90 .

[18] G. Ozaydin- Ince, A. M. Coclite and K. K. Gleason, *Rep. Prog. Phys.,* 2012, **75**, 016501-016541.

[19] G.Ozaydin- Ince, E. Armagan, H. Erdogan, F. Buyukserin, L. Uzun and G. Demirel, ACS Appl. Mater. Interfaces, 2013, **5**, 6447-6452.

[20] G. Ozaydin- Ince, G. Demirel, K. K. Gleason and M. C. Demirel, *Soft Matter,* 2010, **6**, 1635-1639.

[21] G. Ozaydin-Ince, K. K. Gleason and M. C. Demirel, *Soft Matter,*2011, **7**, 638-643.

[22] E. Armagan, Q. Parveen and G. Ozaydin-Ince, *Nanoscience and Nanotechnology Letters,* 2015, **7,** 79-83.

[23] X. Li and H. ShamsiJazeyi, S. L. Pesek, A. Agrawal, B. Hammouda and R. Verduzco, *Soft Matter,* 2014,**10**, 2008-2015 .

[24] K. Tauer, D. Gau, S. Schulze, A. Völkel and R. Dimova, *Colloid Polym. Sci.,* 2009, **287**, 299-312.

[25] M. Heskins and J. E. Guillet, *J. Macromol.Sci, Part A: Pure Appl. Chem.,* 1968, **2,** 1441-1455.

[26] A. C. Lima, W. Song, B. Blanco-Fernandez, C. Alvarez-Lorenzo, and J. F. Mano, *Pharm. Res*., 2011, **28**, 1294-1305.

[27] Z. Shen, W. Wei, Y. Zhao, G. Ma, T. Dobashi, Y. Maki, Z. Su, and J. Wan, *European Journal of Pharmaceutical Science,*2008, **35**, 271-282.

[28] X. Zhang, D. Wu, and C. Chu, *Biomaterials*, 2004, **25**, 3793-3805.

[29] Y. Y. Li, X. Z. Zhang, J. L. Zhu, H. Cheng, S. X. Cheng, and R. X. Zhuo, *Nanotechnology,*2007, **18**, 215605-215612.

[30] Y. Gao, Y. Zhou, and D. Yan, *Polymer,* 2009, **50**, 2572-2577.

[31] K. Cai, F. Jiang, Z. Luo, and X. Chen, *Advanced Engineering Materials,* 2010, **12**, 565-570.

[32] G. Chen, R. Chen, C. Zou, D. Yang and Z. S. Chen, *J. Mater. Chem.,* 2014, **2**, 1327-1334.

[33] H. Dong, and W. E. Jones, Jr., *Langmuir,* 2006, **22**, 11384-11387.

[34] Y. Zhu, L. Feng, F. Xia, J. Zhai, M. Wan, and L. Jiang, *Macromol. Rapid Commun.,* 2007, **28**, 1135-1141.

[35] A. L. Yarin, E. Zussman, J. H. Wendorff, and A. Greiner, *J. Mater. Chem.,*2007, *1*7, 2585-2599.

[36] J.Wang, A. Sutti, X. Wang and T. Lin, *Journal of Colloid and Interface Science*, 2012, 369, 231-237.

[37] C. G. Gomez, C. I. Alvarez, and M. C. Strumia, *Journal of Biochemical and Biophysical Methods,*2003, **55**, 23-26.

[38] J. L. Yagüe, and K. K. Gleason, *Soft Matter,* 2012, **8**, 2890-2894 .

[39] C. S. Brazel, and N. A. Peppas, *Macromolecules,*1995, **28**, 8016-8020.

[40] S. H. Baxamusa, L. Montero, J. M. Dubach, H. A. Clark, S. Borros, and K. K. Gleason, *Macromolecules,*2008, **9**, 2857-2862.

[41] T. Trongsatitkul, and B. M. Budhlall, *Polym. Chem*., 2012, **4**, 1502-1516.

[42] C. Erbil, Y. Yıldız, and N. Uyanık, *Polym. Int.,* 2000, **49**, 795-800.

[43] S. Yarimkaya, and H. Basan, *Journal of Macromolecular Science Part A: Pure and Applied Chemistry,*2007, **44**, 939-946.

[44] K. Tauer, A. M. Imroz Ali, and M. Sedlak, *Colloid. Polym. Sci.,*2005, **283**, 351-358.

[45] C. L. Bell, and N. A. Peppas, *Biomaterials,*1996, **17**, 1203-1218.

[46] A. Asatekin, and K.K. Gleason, *Nano Lett.,* 2011, **11**, 677-686.

TABLES:

Table 1:

		Loading		Release	
Samples	Polymers	pH	Temperature	pH	Temperature
NI1	pNIPAAm	7	25°C	7	25°C
NI2	pNIPAAm	7	40°C	7	25°C
NI3	pNIPAAm	7	25°C	7	40°C
NIHE1	pNIPAAm+pHEMA	7	25°C	7	25°C
NIHE2	pNIPAAm+pHEMA	7	40°C	7	25°C
NIHE3	pNIPAAm+pHEMA	7	25°C	7	40°C
NIMA1	pNIPAAm+pMAA	8	25°C	4	25°C
NIMA2	pNIPAAm+pMAA	8	40°C	4	25°C
NIMA3	pNIPAAm+pMAA	8	25°C	4	40°C

Table 1: Dye loading and release conditions for different samples are shown. NI samples are single layer pNIPAAm nanotubes, whereas NIHE and NIMA are coaxial nanotubes with pNIPAAm outer layer and pHEMA and pMAA inner layers, respectively.

Table 2:

	$\xi \left(\overset{o}{A} \right)$	$\Box$ or (1/ $\Box_s$)	M_c (g/mol)
pNIPAAM (at 40°C)	7.1	1.03	105.67
pNIPAAM (at 25°C)	14.35	1.88	276.98
pHEMA	10.35	8.77	101.66
pMAA (at pH 4)	8.32	1.08	81.88
pMAA (at pH 8)	32.3	2.43	722.62

Table 2: Mesh sizes ξ, swelling ratio $\Box$ and the average molecular weight between the crosslinks M_c of the polymers at different temperature and pH conditions are shown.

FIGURE CAPTIONS:

Figure 1: FTIR spectra of the iCVD deposited crosslinked pMAA, pHEMA and pNIPAAm polymer films are shown. The peak at 3300 cm^{-1} and broad peak between 3150 cm^{-1}-3550 cm^{-1} correspond to the N-H stretching vibration of NIPAAm and O-H stretching vibration of HEMA, respectively. The peak at 1700 cm^{-1} corresponds to the C=O stretching vibration of MAA, whereas C=O stretching vibration of HEMA is at 1730 cm^{-1}.

Figure 2: (a-b) SEM images of the NIMA nanotubes at different length scales are shown. The wall thicknesses of the nanotubes are measured to be approximately 30 nm. The nanotubes can be separated further by centrifuging. The tears observed in some of the nanotubes are due to handling during SEM imaging. (c) SEM images of the NIMA nanotubes with thicker walls are shown. The wall thicknesses of the nanotubes are measured to be approximately 50 nm. (d) SEM images of the NIMA nanotubes with closed ends are shown.

Figure 3: Dye release percentages of (a) NI and control samples, (b) NIHE and (c) NIMA samples under different loading and release conditions are shown. The highest release percentages are observed with NI3, NIMA3 and NIHE3 samples. The dotted lines show the fits to an empirical formula.

Figure 4: Percentage releases obtained at the end of cyclic release studies of (a) NI3, (b) NIHE3 and (c) NIMA3 samples are demonstrated. Maximum of 9% release after three consecutive experiments is observed for all samples.
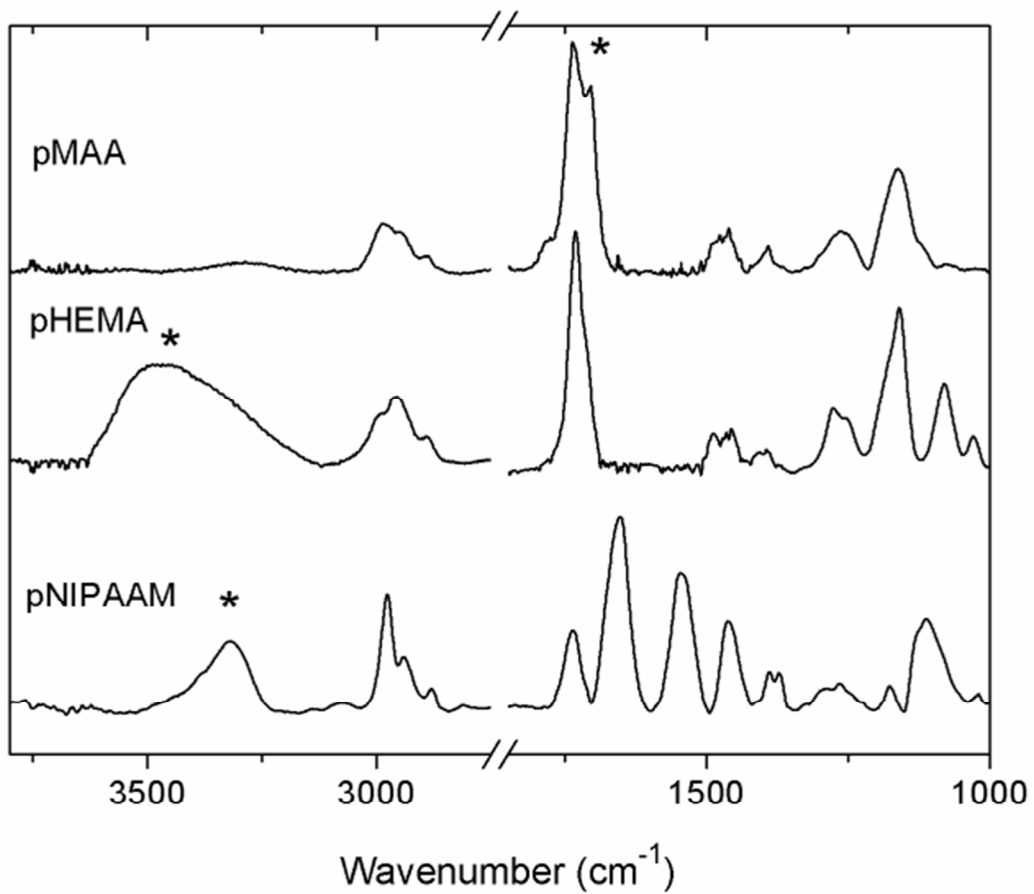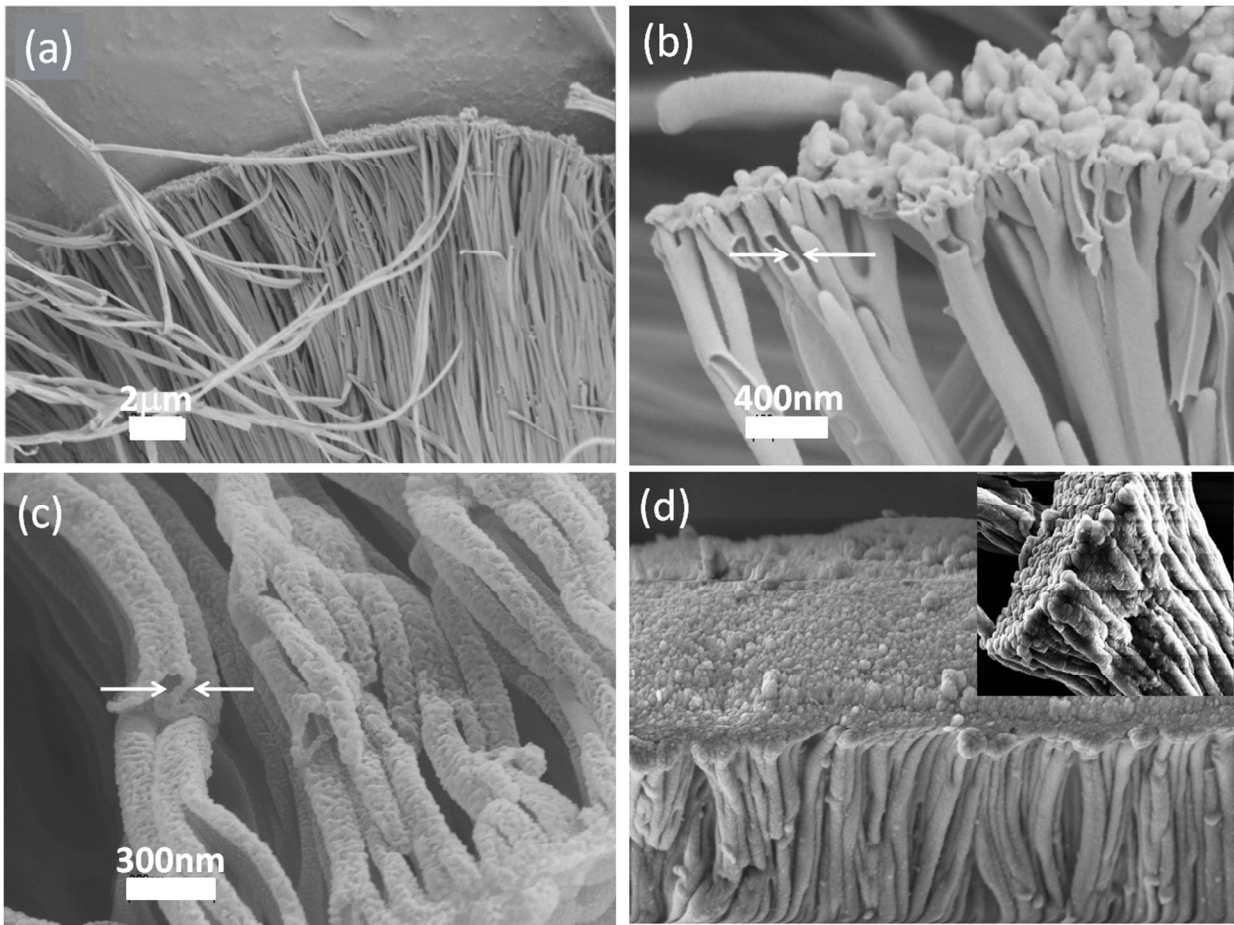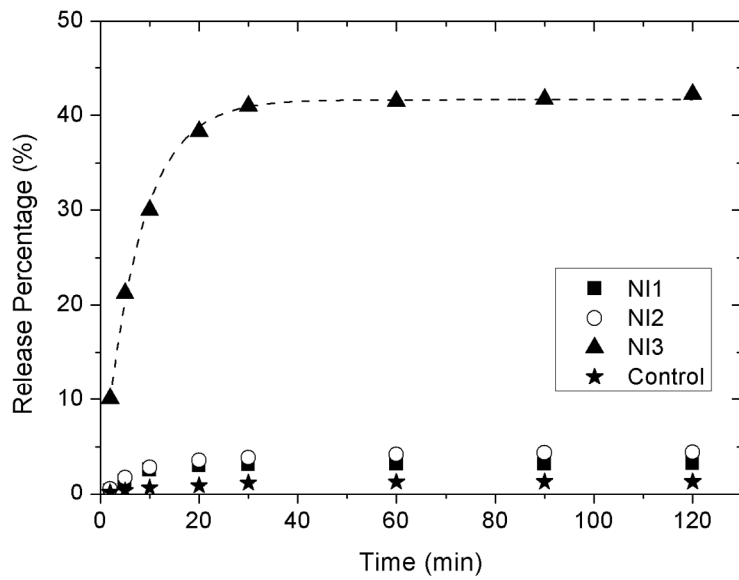
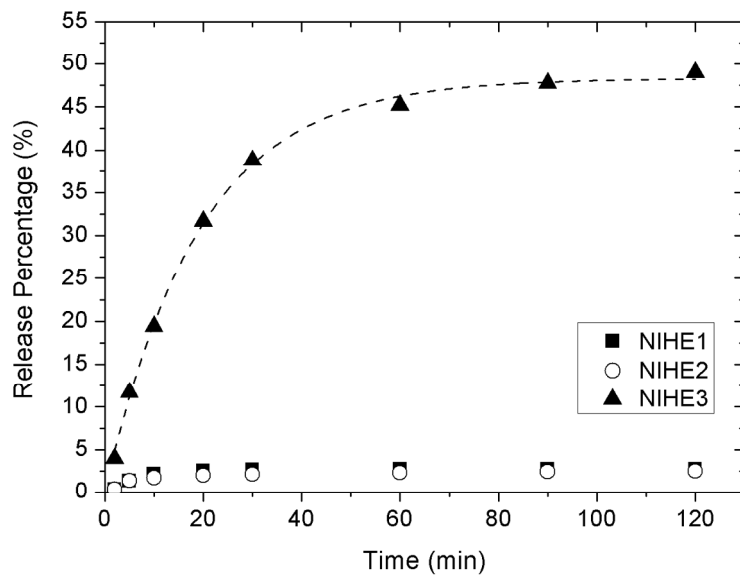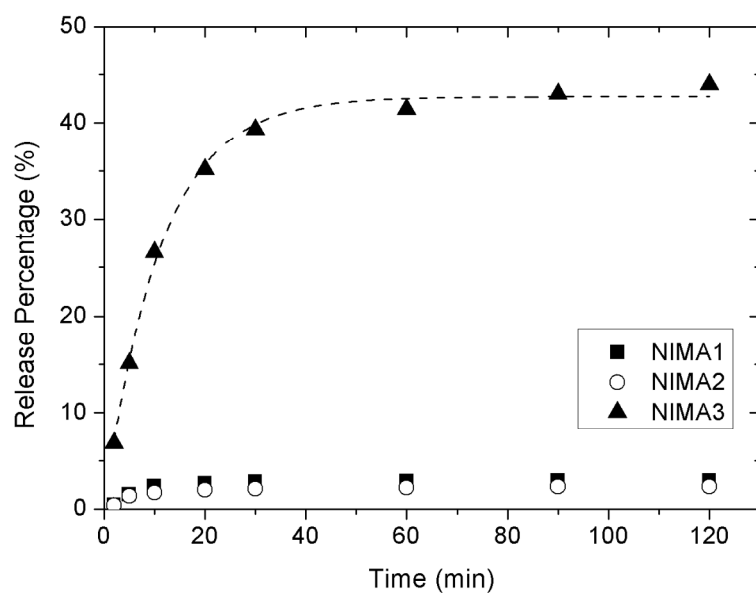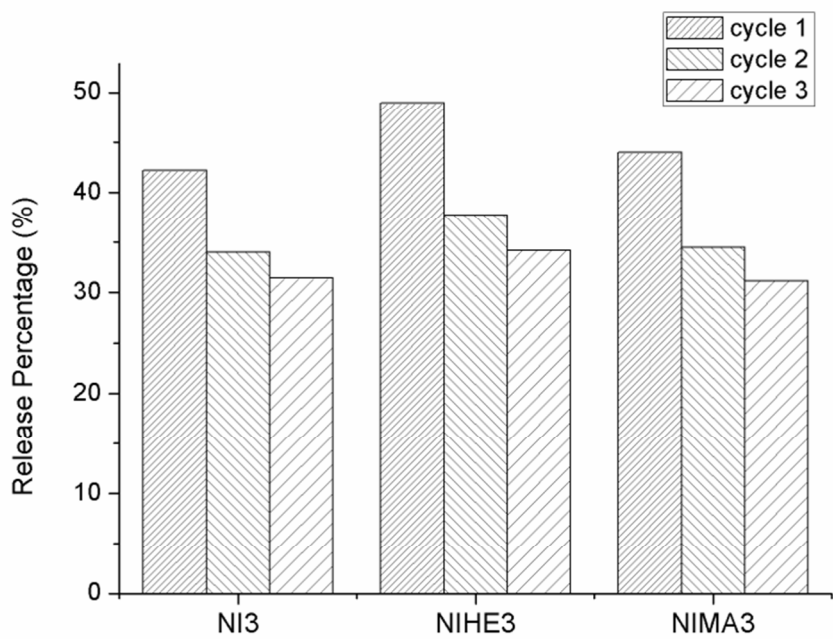**FIGURES:**

Figure 1:

Figure 2:

Figure 3:

(a)

(b)

Figure 3:

(c)

Figure 4:

Title: Coaxial Nanotubes of Stimuli Responsive Polymers with Tunable Release Kinetics

Authors: Efe Armagan, Gozde Ozaydin Ince

Coaxial nanotubes with different stimuli responsive polymer layers demonstrate triggered response with release rates that can be controlled by tuning the polymer chemistry.